

Evidence for Multiple Types of Post-Starburst Galaxies

Emma W. Nielsen^{1,2}, Charles L. Steinhardt^{2,3}, Mathieux Harper³, Conor McPartland^{1,4}, and Aidan Sedgewick^{1,2}

¹ Niels Bohr Institute, University of Copenhagen, Jagtvej 155A, DK-2200 Copenhagen N

² Dark Cosmology Centre (DARK)

³ Department of Physics and Astronomy, University of Missouri, 701. S. College Ave., Columbia, MO 65203

⁴ Cosmic Dawn Center (DAWN)

March 21, 2025

ABSTRACT

The quenching mechanisms of galaxies are not yet fully understood, but post-starburst galaxies provide one explanation for the rapid transition between star-forming and quiescent galaxies. It is generally believed that the starburst initiating the post-starburst phase is merger-driven, however, not all post-starburst galaxies show evidence of a merger, and recent studies suggest that post-starburst galaxies may be produced by multiple distinct mechanisms. This study examines whether multiple types of post-starburst galaxies actually exist — i.e. whether the properties of post-starburst galaxies are multimodal — using Uniform Manifold Approximation and Projection (UMAP) to cluster post-starburst galaxies based on spectroscopic data. It is suggested that there are three types of post-starburst galaxies, which have dissimilar stacked spectral energy distributions and are separated by their $H\alpha/[OII]_{\lambda 3727}$ absorption with an accuracy of 91%. A comparison of various galaxy properties (e.g., emission line strengths, mass and age distributions, and morphologies) indicate that the grouping is not just an age sequence but may be correlated to the merger-histories of the galaxies. It is suggested that the three post-starburst galaxy types have different origins, some of which may not be merger-driven, and that all typical galaxies go through the post-starburst phase at turnoff.

Key words. galaxies: evolution — stars: luminosity function, mass function — stars: formation

1. Introduction

Post-starburst (PSB) galaxies are a class of galaxies selected to have a large population of A stars (traced by $H\delta$), but no O and B stars (traced by $H\alpha/[OII]$). This abundance of A stars is typically interpreted as indicating that PSB galaxies have experienced a recent burst in star formation, whereas the absence of short-lived O and B stars suggests that they have minimal current star formation. Thus, a natural explanation, and the basis for the term post-starburst, is that PSB galaxies have rapidly quenched following an unsustainable burst of star formation (e.g., Vergani et al. 2009; Wilkinson et al. 2017; French 2021).

Because PSB galaxies exhibit an overabundance of galaxy-galaxy mergers, these mergers are a likely candidate for triggering the starbursts that lead to a subsequent PSB phase. A plausible mechanism is that mergers cause dense gas to compress and thereby allow an abrupt increase in star formation, but the detailed mechanisms for producing PSB galaxies are not yet fully understood (Pawlik et al. 2019; French 2021; Li et al. 2023).

Moreover, not all PSB galaxies show evidence of a past or ongoing merger (Pawlik et al. 2015; French 2021; Cheng et al. 2024). This could be due to the morphological evidence of the merger fading over time (Pawlik et al. 2015; French 2021), or alternatively, that there are multiple types of PSB galaxies mixed together — some that are merger-driven and some that are not. Indeed, Li et al. (2023) find that significantly more post-merger PSB galaxies quench their star formation outside-in, whereas slightly more non-post-merger PSB galaxies quench inside-out. Unless some feedback mechanism causes inside-out-quenching galaxies to subsequently quench outside-in, this observation is consistent with the idea that PSB galaxies are produced by multiple distinct mechanisms.

Even if the PSB phase is entirely merger-driven, Pawlik et al. (2019) propose three distinct merger-driven mechanisms which could produce different classes of PSB galaxies. These include a transition from star-forming to quiescent, in which a merger-induced starburst is rapidly quenched; a scenario where the galaxy resumes its star formation after the PSB phase; and a scenario where a quiescent galaxy is rejuvenated by a minor merger. Alternatively, Steinhardt (2024) proposes a secular phase in which galaxies stop forming O and B stars but continue to form low-mass stars, including A stars. These galaxies — termed red star-forming galaxies (RSFGs) — would therefore be selected as PSB, despite not being associated with a starburst or merging. On the other hand, Wilkinson et al. (2017) suggest that variations in PSB selection criteria (which affect other parameters such as color, morphology and the environment) are merely caused by observing the galaxies in different stages of the PSB phase.

If this hypothesis is true and there are populations of PSB galaxies with distinct origins, these populations could have other distinct properties. For example, a rejuvenated galaxy should be as old and as massive as a quiescent galaxy, whereas a galaxy transitioning from star-forming to quiescent should have a mass similar to those at turnoff. Likewise, a secularly evolving RSFG should be less morphologically disturbed than a PSB galaxy whose starburst was initiated by a major merger.

In this work, observational PSB catalogs are used in an attempt to determine whether there are indeed multiple classes of PSB galaxies. The results indicate that there are three spectroscopic classes of PSB galaxies with dissimilar properties. Then, other properties are used to determine if the grouping is due to the galaxies having different origins.

In § 2, the galaxy sample and data are described, and in § 3, these are used to determine whether there are multiple types of PSB galaxies — i.e., whether their properties are multimodal — using machine learning to cluster PSB galaxies based on spectroscopic data. Various galaxy properties (e.g., emission line strengths, mass and age distributions and morphologies) are examined in § 4 to determine the origins of the proposed types of PSB galaxies in § 5. Specifically, three hypothesis are evaluated: (1) the grouping could be an evolutionary sequence; (2) the groups could be produced by mergers affecting different types of precursor galaxies; or (3) some galaxies might instead evolve secularly through the PSB phase. The results are discussed in § 6, finding that this final scenario is most consistent with observations. These results even allow the possibility that PSB galaxies are a turnoff mechanism from the star-forming main sequence, in which case all typical galaxies would go through a PSB phase at turnoff.

2. Galaxy Sample and Data

This work primarily relies on a sample of 2665 PSB galaxies from Meusinger et al. (2017). The catalog includes PSB galaxies with median redshift $z = 0.13$ (16th and 84th percentiles of 0.069 to 0.199) that have been recorded in Stripe 82 by the Sloan Digital Sky Survey Data Release 7 (SDSS DR7, Abazajian et al. 2009). The Meusinger et al. (2017) galaxies are selected to have equivalent widths $EW(H\delta) > 3 \text{ \AA}$, $EW(H\alpha) > -5 \text{ \AA}$ and $EW([OII]) > -5 \text{ \AA}$, where negative values indicate emission and positive values indicate absorption. Thus, the galaxies have strong $H\delta$ absorption and almost no $H\alpha$ or $[OII]$ emission. The use of $H\alpha$ reduces contamination from dust, but may introduce a bias against galaxies with strong narrow-line AGN, strong shocks (which can be expected post-merging), or that are not yet fully quenched (French 2021; Li et al. 2023).

The Meusinger et al. (2017) catalog provides equivalent widths (EWs) of $H\alpha$, $H\delta$, $[OII]\lambda 3727$ and $[OII]\lambda 3729$. Spectral energy distributions (SEDs) are retrieved from the SDSS DR7 Data Archive Server, and the galaxy images used in this work are taken by the Panoramic Survey Telescope and Rapid Response System (Pan-STARRS, Chambers et al. 2019). For each galaxy, photometric stellar masses and star formation rates estimated from nebular emission lines are retrieved from the MPA-JHU catalog (Kauffmann et al. 2003a; Brinchmann et al. 2004). Photometric stellar masses, ages and extinction as well as EWs of $H\alpha$, $H\beta$, $[NII]$ and $[OIII]$ are retrieved from the Portsmouth catalog (Maraston et al. 2013). The MPA-JHU and Portsmouth catalogs include 2647 and 2568 of the Meusinger et al. (2017) galaxies, respectively.

3. Identifying Dissimilar Types of PSB Galaxies

Dissimilar groups of PSB galaxies can be identified using Uniform Manifold Approximation and Projection (UMAP, McInnes et al. 2020). UMAP is an unsupervised machine learning algorithm that performs dimensionality reduction, embedding high-dimensional data in a lower-dimensional space (usually 2D) whilst preserving most of its topological structure. Here, UMAP is provided with EWs of $H\alpha$, $H\delta$, $[OII]\lambda 3727$ and $[OII]\lambda 3729$ — i.e., the strengths of the spectral lines used to select the galaxies — and is given no information about any other galaxy property.

UMAP first approximates the topological structure of the data by constructing a graph that connects every galaxy to its k nearest neighbors and weighs the connections based on how

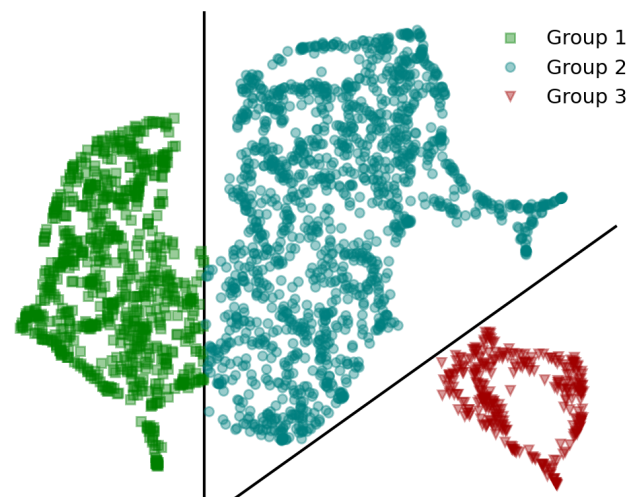


Fig. 1. An arbitrary UMAP embedding of the galaxies in the Meusinger et al. (2017) catalog. Each point represents one galaxy and has opacity $\alpha = 0.4$ to visualize densities. UMAP is provided with EWs of $H\alpha$, $H\delta$, $[OII]\lambda 3727$ and $[OII]\lambda 3729$, and default UMAP parameters are used. The completely disjoint Group 3 ($N = 328$) is visually identified and separated. It is decided to separate Groups 1 ($N = 831$) and 2 ($N = 1506$) due to a bimodality of their $H\alpha$ absorption/emission, see Fig. 2 for further details. The groups can be separated by their EWs of $H\alpha$ and $[OII]\lambda 3727$ with a global accuracy of 91%. This grouping is used throughout this work.

similar the galaxies are (McInnes et al. 2020). Importantly, the weighted graph allows for disjoint groups to exist. UMAP then returns a 2D-embedding of the data where similar galaxies are attracted, and dissimilar galaxies are repelled. Consequently, the dimensions of the UMAP embedding have no physical meaning; rather, galaxies positioned close to each other should be interpreted as similar and vice versa (McInnes et al. 2020), but the precise locations are neither meaningful nor static when the data are provided in a different order.

Fig. 1 shows a UMAP embedding of a single run, where a completely disjoint cluster of galaxies — termed Group 3 — is identified. Because Group 3 is completely disjoint, it should be interpreted as a separate group of PSB galaxies with the strong possibility of having a distinct astrophysical origin. Further, Fig. 2 shows a clear bimodality of $EW(H\alpha)$, suggesting that the remaining galaxies should be divided into Groups 1 and 2, even though these are only partially separated in the UMAP embedding. Pairwise Kolmogorov-Smirnov (KS) tests comparing the univariate distributions of the EWs show that Groups 1 and 2 are inconsistent with being identical ($p \ll 0.01$), supporting the conclusion that these are separate groups. In fact, the groups can be separated by the strengths of their $H\alpha$ and $[OII]\lambda 3727$ emission/absorption with a global accuracy of 91%. Using accuracy as a measure of the performance of the separation criteria is, however, biased, since the distribution of galaxies between the groups is unbalanced.

It should be noted that UMAP uses stochastic processes when searching for the k nearest neighbors and the optimal 2D-embedding. This results in differences in the 2D-embedding from run to run (McInnes et al. 2020) with the possibility that individual objects might switch to a different group (Steinhardt et al. 2023). However, the structural changes between the 16 randomly selected UMAP embeddings shown in Fig. 3 are negligible, and it is qualitatively assessed that UMAP groups the galaxies similarly for a variety of k -values.

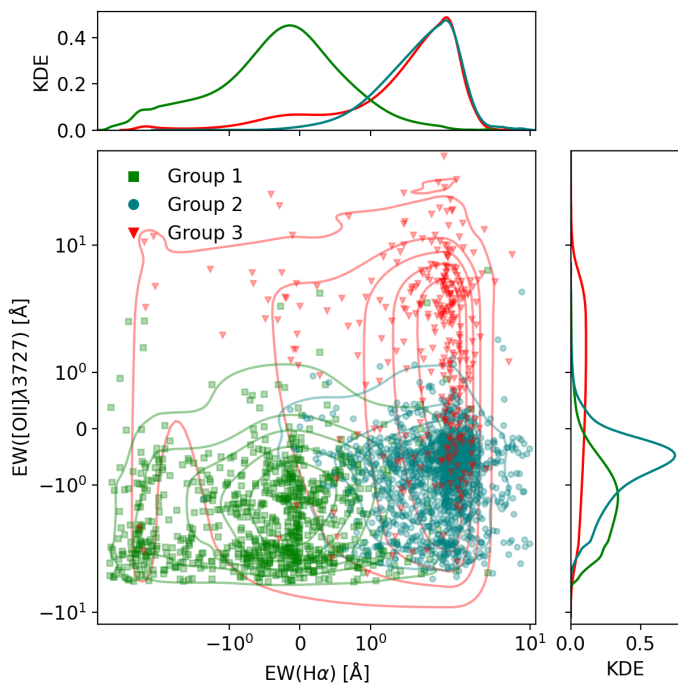


Fig. 2. Kernel density estimates (KDEs) of $EW(H\alpha)$ vs. $EW([OII]\lambda 3727)$ for each group. Negative values indicate emission, and the data are shown on a symmetric logarithmic scale. To ensure that the distributions are depicted accurately, the KDE for Group 2 is limited to $EW(H\alpha) < 10 \text{ \AA}$, including $\geq 98\%$ of the galaxies in this group. The distribution of $EW(H\alpha)$ is clearly bimodal, separating Group 1 from Group 2 and 3. As a result, Groups 1, 2 and 3 are located in different regions of the $EW(H\alpha)$ vs. $EW([OII]\lambda 3727)$ parameter space.

Groups 1, 2 and 3 contain 831, 1506 and 328 PSB galaxies, respectively.

4. Properties of PSB galaxy types

4.1. Spectral Energy Distributions

Table 1 provides an overview of selected spectral properties of the three proposed types of PSB galaxies. Generally, Group 1 emits both $H\alpha$ and $[OII]$, whereas Group 2 emits some $[OII]$, but absorbs $H\alpha$. Group 3 absorbs both $H\alpha$ and $[OII]$.

Fig. 4 shows that Group 1 also emits $[OIII]$ and $[NII]$. This is indicative of ongoing star formation or AGN activity (possibly initiated by merging) (Baldwin et al. 1981; Kewley et al. 2013). Given its strong emission lines, Group 1 could contain AGNs, but following Kauffmann et al. (2003b), many of the galaxies are not classified as AGN. Furthermore, Fig. 5 shows that the groups are not separated in a BPT diagram, indicating that AGN activity does not cause this grouping of PSB galaxies.

The galaxy spectra primarily differ in their spectral lines, but the flux ratios in Fig. 4 show that Group 1 has greater continuum emission in both ends of the visible spectrum. This indicates that Group 1 is dustier than Groups 2 and 3. Conversely, Groups 2 and 3 have gradually weaker emission lines (some of which are replaced by absorption lines) and similar continua, presumably because their O and B stars have died and the dust has been consumed. Extinction measurements are, however, consistent with all three groups being identical. This is somewhat contradictory, but could be explained if Group 2 and/or 3 were slightly redder.

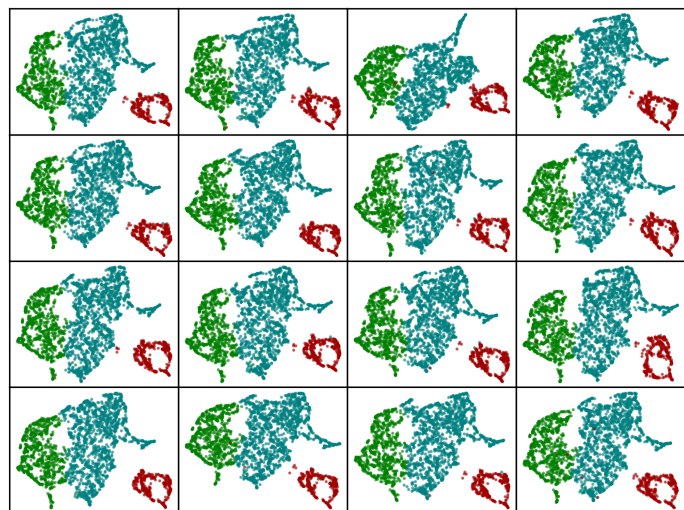


Fig. 3. UMAP embeddings of the galaxies in the Meusinger et al. (2017) catalog sorted randomly into 16 different orders. As in Fig. 1, galaxies in Groups 1, 2 and 3 are colored green, blue and red, respectively. Although the actual locations of the galaxies differ, the structural changes are small, and only a few galaxies jump between groups. The separation appears insensitive to random seeds or the choice of hyperparameters, and instead indicates a true separation into multiple classes.

4.2. Morphologies and Merger Histories

The merger histories of PSB galaxies give insight into the mechanisms producing them, including whether the PSB phase is externally or internally triggered. Although the process of merging disturbs the morphology of the involved galaxies, it is, however, challenging to constrain the merger history of a galaxy. Usually, this is done either by visual inspection or by determining quantitative morphological parameters that are suggestive of past or ongoing mergers (Pawlik et al. 2015; Lotz et al. 2008a).

To examine whether the grouping is correlated to the merger histories of the galaxies, several quantitative morphological parameters have been compared between the groups. These include CAS-statistics, Gini/M20, χ^2 of Sersic fits (e.g., Lotz et al. 2004; Pawlik et al. 2015) and merger probabilities calculated from visual classifications by non-experts in Galaxy Zoo (Willett et al. 2013). The properties are not clearly divided between the groups, but Fig. 6 shows a variation in the asymmetry parameter, which is measured from galaxy images using Statmorph (Rodríguez-Gomez et al. 2018) and quantifies the rotational symmetry of the light from the galaxy (Lotz et al. 2004). On average, Group 3 is less asymmetric than Groups 1 and 2, and KS tests show that Group 3 is inconsistent with being identical to Groups 1 and 2. Thus, Group 3 is probably either associated with a minor merger or no merger at all.

Li et al. (2023) present a different catalog of PSB galaxies that are visually classified as either post-merger or non-interacting (and thereby non-post-merger). This is done following the methodology in Nair & Abraham (2010), where post-mergers are found among galaxies with unusual forms in their g-band images. The Li et al. (2023) galaxies are selected to have statistically similar stellar masses and redshifts (in the range $0.02 \leq z \leq 0.06$). Requiring $EW(H\delta) > 3 \text{ \AA}$, $EW(H\alpha) > -10 \text{ \AA}$ and $\log(-EW([OII])) < 0.23 \times EW(H\delta) - 0.46$, the catalog includes 264 resolved PSB galaxies, 96 of which are identified as post-merger.

Although the Li et al. (2023) PSB sample is too small to reliably identify any groups in a UMAP embedding, some struc-

	Group 1	Group 2	Group 3
EW(Hα) [Å]	-0.28 (-1.91 to 0.45)	2.26 (1.48 to 3.27)	2.14 (1.19 to 2.82)
EW(Hδ) [Å]	5.47 (3.85 to 7.44)	4.40 (3.35 to 6.39)	3.96 (3.28 to 5.69)
EW([OII]λ3727) [Å]	-1.74 (-3.19 to -0.75)	-0.65 (-1.59 to -0.23)	1.94 (-0.25 to 5.96)
EW([OII]λ3729) [Å]	-2.02 (-3.57 to -0.90)	-0.77 (-1.72 to -0.25)	1.01 (-1.04 to 5.84)

Table 1. Median EWs of selected spectral lines for the identified PSB groups from the Meusinger et al. (2017) catalog (16th and 84th percentiles shown in parentheses). All PSB galaxies in the catalog have strong H δ absorption. In addition, Group 1 emits some H α and [OII], whereas Group 2 absorbs H α , but emits some [OII]. Group 3 absorbs both H α and [OII].

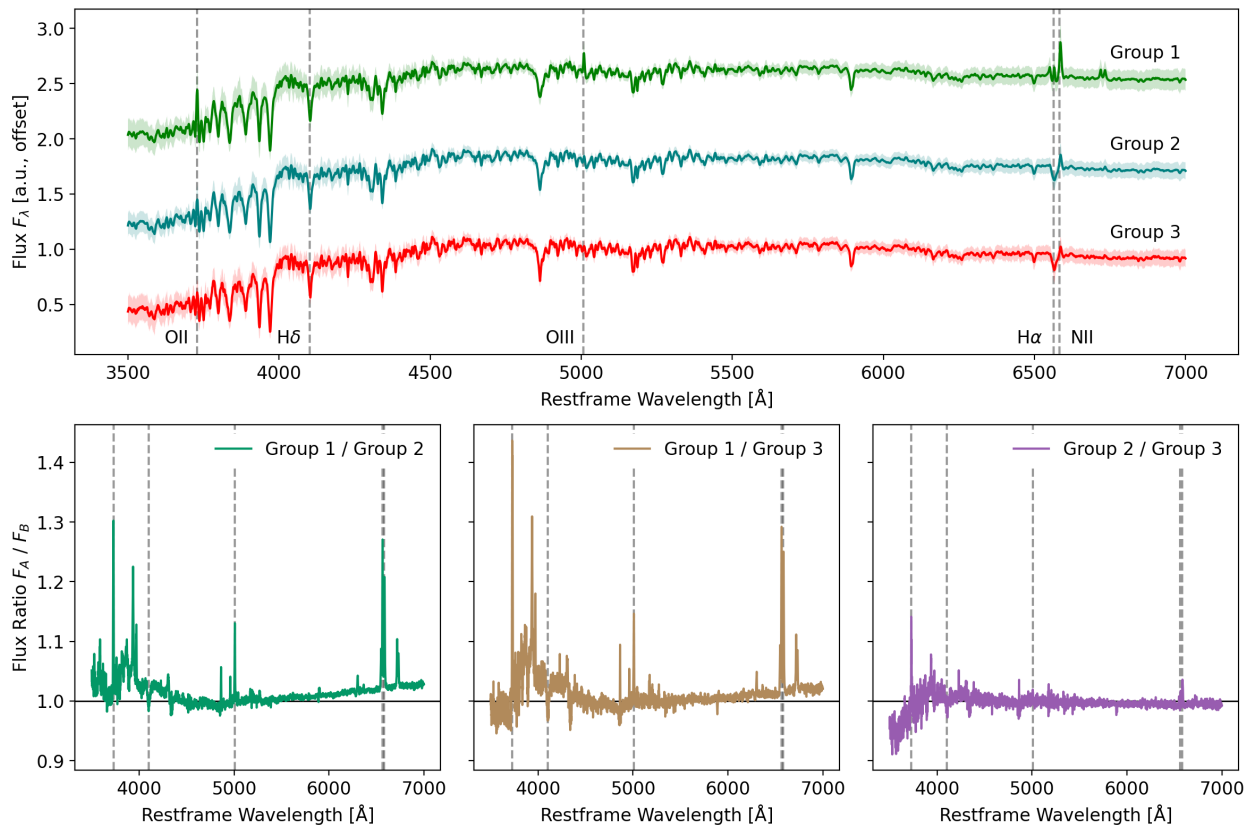


Fig. 4. *Top:* Stacked SEDs for the PSB groups identified in the Meusinger et al. (2017) catalog. Groups 1, 2 and 3 are shown from top to bottom. Prior to stacking, the SEDs have been normalised by the mean flux in the 5050-5150 Å region to account for redshift dependencies (identical continua have been assumed). All SEDs are given equal weight, but only spectra with a signal to noise ratio > 5 for both g-, r- and i-bands are included (this includes > 97% of the galaxies in the catalog). 16th and 84th percentiles are shown within the shaded area, and selected spectral lines are highlighted. The groups share many spectral features but, e.g., differ by the properties shown in table 1. Group 3 also differs by, e.g., emitting [OII] and [NII]. *Bottom:* Flux ratios. Group 1 has stronger spectral lines and greater continuum emission, especially towards lower and higher wavelengths, indicating that its galaxies are dustier. Groups 2 and 3 have similar continua and spectral lines with some deviations towards lower wavelengths.

tures can still be studied. In fact, UMAP embeddings of the Li et al. (2023) galaxies suggest that the spectral properties of a PSB galaxy are correlated to its merger history: If there were no correlation between the merger history of a galaxy and its spectral properties, the post-mergers should be randomly distributed across the embedding, because UMAP is given no information about any morphological features of the galaxies. Thus, the fraction of post-mergers in any sufficiently large section should be similar to that of the entire catalog. However, in a selected region that includes 25% of the galaxies in the catalog and 50% of the post-mergers, 71% are post-merger — as opposed to the expected 36% if the post-mergers were randomly distributed. This excess factor of two indicates that post-merger PSB galaxies share some spectral properties that separate them from non-post-

merger PSB galaxies. This is consistent with there being multiple types of PSB galaxies and multiple mechanisms for quenching star formation. Because merger histories are difficult to constrain, the post-merger fraction in the selected region could be even larger. Similarly, Ventou et al. (2019) suggest a merger fraction of $\sim 20\%$ for galaxies at redshift $z < 1.5$, which is comparable to the merger fraction of 25% among the remaining galaxies.

4.3. Derived Properties

Additional, derived galaxy properties can be used to evaluate potential explanations for the origins of these three groups. In principle, these derived properties could have been used to produce the embedding described in § 3. However, they are measured

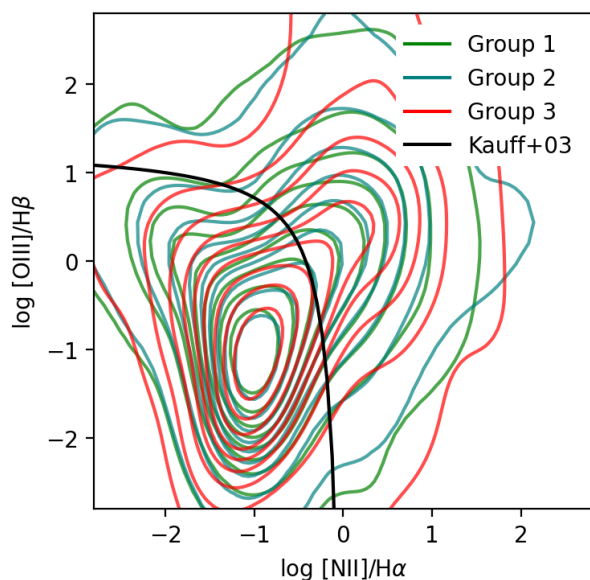


Fig. 5. Contour BPT diagrams of the three PSB groups. Galaxies above the black line are classified as AGN cf. Kauffmann et al. (2003b). Many of the PSB galaxies are not AGN, and the contours are similar for all three groups, indicating that AGN activity does not cause this grouping.

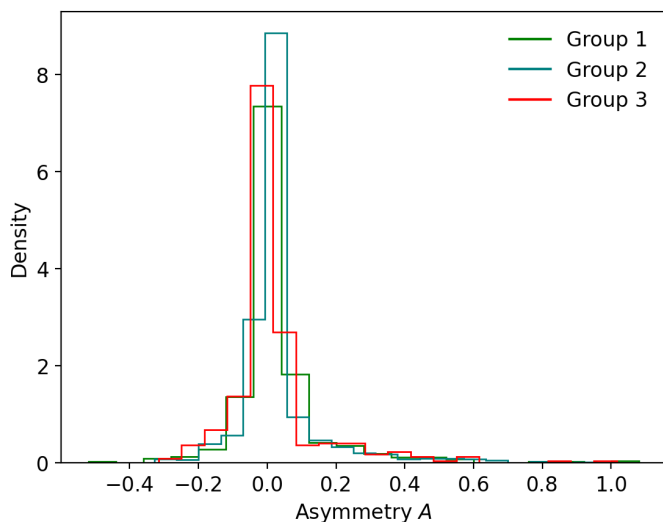


Fig. 6. Asymmetry distributions for the three PSB groups in the Meusinger et al. (2017) catalog. The asymmetry parameter is measured using Statmorph, following the methodology of Lotz et al. (2004). KS tests show that Group 3 is inconsistent with being identical to Groups 1 and 2 ($p < 0.01$), whereas Groups 1 and 2 are only weakly inconsistent with being identical ($p \sim 0.017$). Group 3 has a smaller mean asymmetry than Groups 1 and 2. These differences could be blurred by poor preprocessing of the images.

via photometric template fitting, and therefore rely on several strong assumptions (e.g., the shape of the star formation history). Further, individual galaxy properties are often only very weakly constrained, so that the most useful results instead come from considering distributions of properties across large galaxy samples (Ilbert et al. 2013; Mitchell et al. 2013; Speagle et al. 2014; Davidzon et al. 2017; Weaver et al. 2023). Thus, it is still meaningful to test whether the groups have similar or dissimilar distributions of derived properties, even though the individual values may not be robust.

Perhaps the most informative are the stellar mass distributions. It has been known for several decades that at fixed redshift, the most massive galaxies are predominantly quiescent, while the least massive are still star-forming, one of several results collectively termed downsizing (cf. Cowie et al. (1996)). Galaxies with stellar masses similar to the most massive star-forming galaxies will be quiescent at lower redshifts, implying that these galaxies must turn off in the near future.

Fig. 7 shows that all three groups of PSB galaxies have masses similar to both the most massive star-forming galaxies and the least massive quiescent galaxies, corresponding to galaxies which should be at or near turnoff. Thus, it would appear that all three groups of PSB galaxies might be associated not with rejuvenation of typical quiescent galaxies, in which case their stellar mass distribution should be more similar to the quiescent stellar mass distribution, but rather with turnoff from the star-forming main sequence. Further, Fig. 8 shows that galaxies within the three PSB groups migrate from the star-forming region (Group 1) to the transitional region (Group 3) on a SFR vs. stellar mass diagram, suggesting the possibility that the three might comprise an age sequence within a single scenario for main sequence turnoff. However, based on ages from the star-forming model in the Portsmouth catalog, galaxies in all three groups are consistent with having identical age distributions ($p > 0.1$).

Groups 1 and 2 have statistically similar mass distributions, whereas Group 3 is skewed towards the low-mass end (Fig. 7). This is true for stellar masses measured by both the MPA-JHU catalog and the Portsmouth catalog. As a result, this deviation is likely genuine, although there is no obvious mechanism that would produce it. One possibility is that Group 3 should actually comprise two groups, and that the limited information provided to UMAP is insufficient to separate them.

5. Potential Origins of PSB Galaxy Types

In § 3 and 4, it has been argued that there are three distinct types of PSB galaxies rather than a single type as has previously been proposed. Here, several possibilities for explaining the origins of these distinct types are considered:

1. The grouping could be an evolutionary sequence where Group 1 is the youngest and Group 3 is the oldest.
2. The groups could all be merger-driven, but produced by different types of mergers.
3. Some of the groups could instead evolve secularly through the PSB phase, such as in the red star-forming galaxy scenario (Steinhardt 2024).

A summary of the results is given in Table 2.

5.1. An Evolutionary Sequence

One interpretation is that the grouping is an evolutionary sequence of PSB galaxies of similar origin. Here, Group 1 is assumed to be the youngest (and Group 3 the oldest) due to the gradual decrease of $H\alpha$ and [OII] emission and SFRs towards Group 3. This is consistent with the canonical picture that PSB galaxies are in the midst of rapidly quenching. Further, Group 1 is dustier and emits some [OIII], indicating that some of its O and B stars have not yet died.

If the PSB phase has been initiated by a merger (as commonly believed), the evidence of the merger will fade over time. If the grouping is an evolutionary sequence, the evidence of the

Measurement	Age Sequence Prediction	Merger-Driven Mechanisms Prediction	RSFG Prediction	Observation
Emission line strengths	Decrease towards Group 3	Decrease towards Group 3	Weak in Group 3	Decrease towards Group 3
Mass distribution	Similar	Group 1-2 like SFGs, Group 3 like QGs	Could be dissimilar	Groups 1-2 similar, Group 3 different
Age distribution	Increase towards Group 3	Higher in Group 3	Could be similar	Similar
Extinction	Decrease towards Group 3			Higher in Group 1
SFR	Decrease towards Group 3		Low in Group 3	Decrease towards Group 3
Asymmetry	Decrease towards Group 3	Lower in Group 3	Low in Group 3	Lower in Group 3

Table 2. Overview of predictions for a selection of proposed models and the observations used to test them. The green, yellow and red cell color indicates that the model is either consistent, weakly (in)consistent or inconsistent with the observations, respectively.

merger should therefore be less pronounced in Group 3. This is consistent with observations, as Group 3 is less asymmetric than Group 1. The partial separation of post-mergers and non-post-mergers in the Li et al. (2023) catalog is also consistent with the grouping being an evolutionary sequence of merger-driven PSB galaxies: Obvious post-mergers and non-post-mergers are easily categorized, whereas recovered post-mergers may be wrongly categorized as non-post-mergers. Likewise, the size of the merger may affect the extent to which the morphology of the galaxy is disturbed, causing variations in the asymmetry parameter (Lotz et al. 2008b).

However, observations indicate that the galaxies are equally old, suggesting that the grouping is not an evolutionary sequence. On the other hand, it is difficult to determine the age of a galaxy using photometric template fitting (as in this case; cf. Pforr et al. 2012), and a high resolution is needed to differentiate between the ages of galaxies in a short-lived phase like this. Further, this method is dominated by the continuum, whereas the SEDs primarily differ in the lines (Fig. 4).

If the groups comprise an age sequence, they should have nearly identical stellar mass distributions, because they have similar origins and none of them actively form stars. Group 3 has a mass distribution that is statistically different from Groups 1 and 2 (Fig. 7), which would be inconsistent with the age sequence hypothesis. However, the discrepancy is limited to a small fraction of Group 3 on the low-mass end. Thus, another possibility is that Group 3 actually comprises two Groups, one in the low-mass end and one with a mass distribution similar to Groups 1 and 2.

5.2. Distinct Merger-Driven Origins

As shown in § 4, the properties of PSB galaxies are multimodal. Thus, the three groups likely do not constitute a single evolutionary sequence, but instead have distinct astrophysical origins. However, the PSB phase could still be entirely merger-driven.

As described in § 1, Pawlik et al. (2019) present three distinct, merger-driven mechanisms for producing PSB galaxies, differentiated by the evolutionary stage a galaxy is in when the merger occurs. The three groups might then be caused by mergers creating a starburst and subsequent post-starburst phase in star-forming galaxies, turnoff galaxies, and quiescent galaxies.

Since Group 1 has the highest SFR and the strongest emission lines, this group may represent the Pawlik et al. (2019) blue-to-blue cycle in which the galaxies resume their star formation after the PSB phase. Group 2 may include galaxies that transition from star-forming to quiescent, and the low asymmetry of Group 3 suggests that its (formerly quiescent) galaxies may have been rejuvenated by minor mergers. Moreover, Group 3 should have weaker emission lines because its star formation has already quenched, and the minor merger has only caused a weak starburst. This is consistent with the general trend observed in Fig. 8.

If the groups are produced by mergers affecting different types of precursor galaxies, Groups 1 and 2 (originating from star-forming galaxies) should have a mass distribution similar to star-forming galaxies, whereas Group 3 (originating from quiescent galaxies) should have a mass distribution similar to quiescent galaxies. This prediction is consistent with observations, since all three PSB groups have masses similar to both the most massive star-forming galaxies and the least massive quiescent galaxies, see Fig. 7.

Pawlik et al. (2019) further suggest that the blue-to-blue cycle occurs for $\sim 30\%$ of PSB galaxies with $9.5 < \log(M_*/M_\odot) < 10.5$, which is consistent with Group 1 containing $\sim 30\%$ of the galaxies within this mass range. Pawlik et al. (2019) also suggest that $\sim 70\%$ of PSB galaxies with $9.5 < \log(M_*/M_\odot) < 10.5$ and $\sim 60\%$ of PSB galaxies with $\log(M_*/M_\odot) > 10.5$ transition from star-forming to quiescent due to a gas-rich major merger, which is consistent with Group 2 containing $\sim 60\%$ of the galaxies within both of these mass ranges. However, Pawlik et al. (2019) suggest that $\sim 40\%$ of PSB galaxies with $\log(M_*/M_\odot) > 10.5$ are rejuvenated galaxies, whereas Group 3 only contains $\sim 10\%$ of the Meusinger et al. (2017) galaxies within this mass range. Pawlik et al. (2019) also suggest that these galaxies gradually move towards the high-mass end of the red sequence, but Group 3 is found in the low-mass end. Contrary to observations, in this scenario Group 3 is also expected to have an older stellar population, since it was previously quiescent. Instead, the stellar populations in all three groups have similar age distributions.

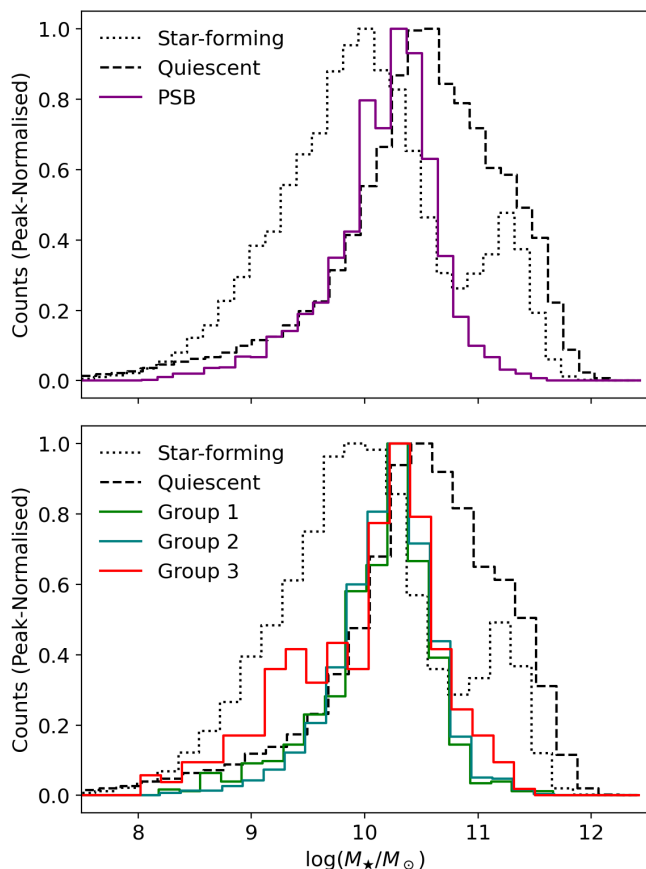


Fig. 7. Stellar Mass distribution of PSB galaxies in the Meusinger et al. (2017) catalog compared to star-forming (SFGs) and quiescent (QGs) galaxies. Stellar masses are taken from the Portsmouth catalog, and the quiescent sample is selected to have $\text{SFR} = 0$. *Top:* The PSB galaxies have masses covering the range from the most massive star-forming galaxies to the least massive quiescent galaxies with a peak in between, suggesting that PSB galaxies are near turnoff. *Bottom:* Groups 1 and 2 are statistically similar ($p > 0.1$), but Group 3 differs ($p \ll 0.01$), predominantly on the low-mass end.

5.3. RSFGs and Secular Evolution

The Pawlik et al. (2019) interpretation might be consistent with observations of Groups 1 and 2, but is seemingly inconsistent with Group 3. A plausible interpretation must be able to explain why the galaxies in Group 3 are the reddest, yet are younger than quiescent galaxies and lie in the low-mass end of the red sequence.

One possibility is that Group 3 contains the non-merger-driven, but secularly evolving red star-forming galaxies proposed by Steinhardt (2024). This interpretation is consistent with Group 3 having weaker emission lines, since RSFGs have stopped actively forming O and B stars. The model also explains why Group 3 has a lower SFR, as SFRs are traced by short-lived O and B stars, not the low-mass stars that RSFGs are still actively forming.

In addition, all three galaxy types could be equally old — as observations suggest — with some evolving secularly and some being forced into the PSB-phase by mergers. Of course, the non-merger-driven Group 3 will have a lower asymmetry as observed.

Finally, the mass distribution of Group 3 — ranging from the most massive star-forming galaxies to the least massive qui-

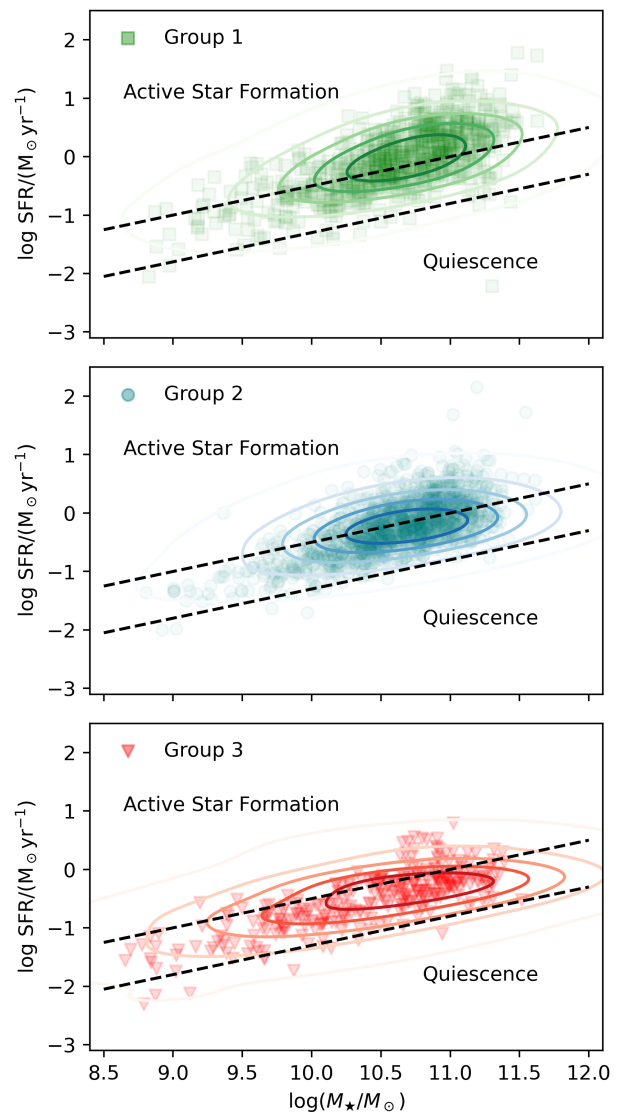


Fig. 8. SFR vs. stellar mass parameter space for each of the PSB groups in the Meusinger et al. (2017) catalog. Groups 1, 2 and 3 are shown from top to bottom. Galaxy properties shown are taken from the MPA-JHU catalog, and the transitional region is outlined by the dashed lines following Li et al. (2023). Galaxies appear to migrate from the active star-forming region (Group 1) to the transitional region (Group 3).

escent ones — is consistent with RSFGs being at turnoff. Further, Group 3 could (but is not required to) have a different mass distribution if it is produced by a different mechanism, which is consistent with its deviation from Groups 1 and 2 on the low-mass end. Steinhardt (2024) makes no additional predictions for the mass distribution of RSFGs compared to merger-driven PSB galaxies.

6. Discussion

Using UMAP to cluster PSB galaxies based on the strengths of selected spectral lines, there is strong evidence that there are three distinct types of post-starburst galaxies with dissimilar origins. It appears that the grouping is not simply an age sequence, but is instead correlated with both additional observed galaxy properties and likely also with the merger histories of these galaxies.

The most likely scenario is that the three types of PSB galaxies have distinct astrophysical origins, some of which may not be associated with a merger or a starburst. Groups 1 and 2 have several properties in common with merger-driven scenarios, but Group 3 appears to be inconsistent. The hypothesis that galaxies might not quench when leaving the main sequence, but rather continue as red star-forming galaxies (RSFG; Steinhardt 2024), is consistent with observations of Group 3.

However, additional falsifiable tests are needed to determine the exact origins of the three PSB galaxy types. Moreover, (for the properties compared in this work) the RSFG hypothesis makes less specific predictions that are harder to reject. Thus, future research could compare the quenching directions of the PSB galaxy types to decide whether the PSB phase(s) are internally or externally triggered: Li et al. (2023) find post-mergers predominantly quench outside-in, whereas RSFGs are expected to quench inside-out (Steinhardt 2024). If there is no correlation between the PSB groups and their quenching directions, the RSFG interpretation must therefore be rejected.

Interestingly, the mass distributions of all three PSB groups range from the most massive star-forming galaxies to the least massive quenched galaxies. This is expected for Group 3, if it contains RSFGs that are at turnoff — the fact that all three PSB galaxy types have masses in this range indicate that they are all near turnoff. This observation is consistent with downsizing, the idea that the most massive galaxies formed the bulk of their stellar mass on a shorter time scale. Similarly, Wong et al. (2012) suggest that PSB galaxies contribute to building up the low-mass end of the red sequence. This is interesting because PSB galaxies are believed to be created by some rare event — but if they are all near turnoff, maybe all typical galaxies go through the post-starburst phase.

Generally, downsizing is inconsistent with any interpretation where the galaxies do not transition from star-forming to quiescent — e.g., the rejuvenation of galaxies or the blue-to-blue cycle interpretation of Group 1 — but the hypothesis does not constrain the quenching mechanism(s) further. Thus, other interpretations may be consistent with downsizing too. However, there would be no reason for post-mergers to be over-represented among PSB galaxies if the majority of galaxies evolve secularly through the PSB phase. Therefore, at least one of the PSB groups is likely to be associated with merging.

Acknowledgements. The authors would like to thank Eva Gregersen, Preethi Nair, Jens Nielsen, Tom Reynolds and Darach Watson for helpful comments. EN, CS, MH, and AS were supported by research grants (VIL16599, VIL54489) from VILLUM FONDEN.

References

Abazajian, K. N., Adelman-McCarthy, J. K., Agüeros, M. A., et al. 2009, *The Astrophysical Journal Supplement Series*, 182, 543–558

Baldwin, J. A., Phillips, M. M., & Terlevich, R. 1981, *Publications of the Astronomical Society of the Pacific*, 93, 5

Brinchmann, J., Charlot, S., White, S. D. M., et al. 2004, *Monthly Notices of the Royal Astronomical Society*, 351, 1151–1179

Chambers, K. C., Magnier, E. A., Metcalfe, N., et al. 2019, *The Pan-STARRS1 Surveys*

Cheng, Z., Li, C., Li, N., Yan, R., & Mo, H. 2024, *The Astrophysical Journal*, 961, 216

Cowie, L. L., Songaila, A., Hu, E. M., & Cohen, J. G. 1996, *The Astronomical Journal*, 112, 839

Davidzon, I., Ilbert, O., Laigle, C., et al. 2017, *Astronomy & Astrophysics*, 605, A70

French, K. D. 2021, *Publications of the Astronomical Society of the Pacific*, 133, 072001

Ilbert, O., McCracken, H. J., Le Fèvre, O., et al. 2013, *Astronomy & Astrophysics*, 556, A55

Kauffmann, G., Heckman, T. M., Simon White, D. M., et al. 2003a, *Monthly Notices of the Royal Astronomical Society*, 341, 33–53

Kauffmann, G., Heckman, T. M., Tremonti, C., et al. 2003b, *Monthly Notices of the Royal Astronomical Society*, 346, 1055–1077

Kewley, L. J., Maier, C., Yabe, K., et al. 2013, *The Astrophysical Journal*, 774, L10

Li, W., Nair, P., Rowlands, K., et al. 2023, *Monthly Notices of the Royal Astronomical Society*, 523, 720–738

Lotz, J. M., Davis, M., Faber, S. M., et al. 2008a, *The Astrophysical Journal*, 672, 177–197

Lotz, J. M., Jonsson, P., Cox, T. J., & Primack, J. R. 2008b, *Monthly Notices of the Royal Astronomical Society*, 391, 1137–1162

Lotz, J. M., Primack, J., & Madau, P. 2004, *The Astronomical Journal*, 128, 163–182

Maraston, C., Pforr, J., Henriques, B. M., et al. 2013, *Monthly Notices of the Royal Astronomical Society*, 435, 2764–2792

McInnes, L., Healy, J., & Melville, J. 2020, *UMAP: Uniform Manifold Approximation and Projection for Dimension Reduction*

Meusinger, H., Brünecke, J., Schalldach, P., & in der Au, A. 2017, *Astronomy & Astrophysics*, 597, A134

Mitchell, P. D., Lacey, C. G., Baugh, C. M., & Cole, S. 2013, *MNRAS*, 435, 87

Nair, P. B. & Abraham, R. G. 2010, *The Astrophysical Journal Supplement Series*, 186, 427–456

Pawlik, M. M., McAlpine, S., Trayford, J. W., et al. 2019, *Nature Astronomy*, 3, 440–446

Pawlik, M. M., Wild, V., Walcher, C. J., et al. 2015, *Monthly Notices of the Royal Astronomical Society*, 456, 3032–3052

Pforr, J., Maraston, C., & Tonini, C. 2012, *MNRAS*, 422, 3285

Rodriguez-Gomez, V., Snyder, G. F., Lotz, J. M., et al. 2018, *Monthly Notices of the Royal Astronomical Society*, 483, 4140–4159

Speagle, J. S., Steinhardt, C. L., Capak, P. L., & Silverman, J. D. 2014, *The Astrophysical Journal Supplement Series*, 214, 15

Steinhardt, C. L. 2024, *Do Red Galaxies Form More Stars Than Blue Galaxies?*

Steinhardt, C. L., Mann, W. J., Rusakov, V., & Jespersen, C. K. 2023, *ApJ*, 945, 67

Ventou, E., Contini, T., Bouché, N., et al. 2019, *Astronomy & Astrophysics*, 631, A87

Vergani, D., Zamorani, G., Lilly, S., et al. 2009, *Astronomy & Astrophysics*, 509, A42

Weaver, J. R., Davidzon, I., Toft, S., et al. 2023, *Astronomy & Astrophysics*, 677, A184

Wilkinson, C. L., Pimblett, K. A., & Stott, J. P. 2017, *Monthly Notices of the Royal Astronomical Society*, 472, 1447–1457

Willett, K. W., Lintott, C. J., Bamford, S. P., et al. 2013, *Monthly Notices of the Royal Astronomical Society*, 435, 2835–2860

Wong, O. I., Schawinski, K., Kaviraj, S., et al. 2012, *Monthly Notices of the Royal Astronomical Society*, 420, 1684–1692